Accurate Intraocular Lens Position Determination in Pseudophakic Eye

Author: Miguel Joana de Sousa Prata,[1]
Supervisors: João Mendanha Dias, PhD,[1] and Filomena Ribeiro, MD, PhD, FEBO[2]
[1] *Instituto Superior Técnico, GoLP*
[2] *Hospital da Luz*
(Dated: April 26, 2016)

A custom-built pseudophakic eye phantom was used to assess the accuracy of two comercial ACD_{post} measuring devices, the Haag-Streit Lenstar LS 900, and the Zeiss Visante OCT. Calibrations were performed for the two devices and the span shift error was found to be virtually inexistent. The thickness of an IOL was measured with the Zeiss Visante OCT and a $56 \pm 25\mu$m error was found, which, considering this to be representative of the zero shift error, is clinically insignificant.

A clinical trial was conducted where biometric data was collected. ACD_{post} measurements were performed with both two devices, the Haag-Streit Lenstar LS 900, and the Zeiss Visante OCT and the results were found to be clinically interchangeable.

Ray tracing was used in conjunction with biometric data collected during the clinical trial to back calculate the ACD_{post}. The spherical equivalent refraction at the spectacle plane was also back calculated, using ACD_{post} measurements from the Zeiss Visante as input parameter. The results obtained were found to be on par with the ones from current IOL power calculation formulas.

I. MOTIVATION

Vision is of major importance for humans. It's a complex and not yet fully understood process: light is converted into electrical pulses in the retina, which are then interpreted by the brain, giving us a perception of our surroundings. Vision quality depends, not exclusively, on the quality of the image arriving at the retina and cataracts are a cause of degradation of the quality of said image.

A cataract is an opacification of the crystalline lens[1], resulting in impaired vision and, in severe cases, blindness, having to be surgically removed in order to restore vision. This condition is usually developed through aging and according to the World Health Organization (WHO) is the world's leading cause of blindness [1].

Primarily, in cataract surgery, the opacified lens was simply removed, which resulted in a severely hypermetropic eye, lacking dioptric power. Patients would afterwards be prescribed spectacles with lenses powerful enough to compensate for this. Nowadays the standard cataract surgery technique is phacoemulsification: the opaque crystalline lens is gradually destroyed and extracted, followed by the implantation of an Intraocular Lens (IOL). The IOL should have an adequate power, compensating the loss of the crystalline lens and, ideally, providing a spectacle free postoperative experience. Despite the progress that this area observed in the last decades approximately 20% of patients, depending on their eye's axial length, still require a refractive correction of more than $\pm$0.5D post-operatively [2]. Due to the demographic trend of longer lifespans it is also expected to see a twofold increase in the number of people requiring cataract surgery, from 20 million cases in 2010 to 40 million in 2020 [3]. This combination of factors makes the issue of accurate IOL power calculation one of major importance.

[1] The crystalline lens is an optical element of variable refracting power, allowing focus to be achieved at different distances – a process known as accommodation.

II. STATE OF THE ART

Currently the power of the implanted IOL is calculated with formulas derived by retrospective analysis of a large number of patients who had IOL implantation, and whose data was subjected to regression analysis, resulting in a power calculation formula, characterized by a set of constants which are calculated so that the postoperative refractive error, given by the difference between the target and postoperative refraction, averages zero. These formulas relate several biometric parameters measured preoperatively, such as the corneal power and the axial length of the eye, in order to calculate the power of the IOL. Another parameter taken into consideration when calculating the power is the Effective Lens Position (ELP)[2], which acts as proxy to the physical position of the IOL inside the eye, given by the Postoperative Anterior Chamber Depth (ACD_{post}). This estimate is of a major importance to the refractive outcome with errors in its estimation having a 42% relative contribution to the total refractive error, contrasting with a 36% relative contribution of axial length measurement errors and 22% relative contribution of corneal power measurement errors, [4].

Due to the difficulty in effectively predicting ACD_{post} several authors have explored the possibility of using the symmetry of the eye in order to improve the refractive outcome [5–7]. By performing the surgery sequentially the refractive outcome of the first operated eye is assessed and its ACD_{post} measured. The power of the IOL to be implanted in the other eye is calculated considering these parameters which results in an improved refractive outcome, compared with calculating the power of each IOL independently. This technique was shown to be more effective when the corneal power of the two eyes was similar (a corneal power difference smaller than 0.6D between the eyes) [8].

[2] Distance from the anterior cornea to the IOL when this is modeled as having a null thickness.

Currently there is a need to assess the accuracy of ACD_{post} measurement techniques, which is evidenced by the significant discrepancies among the results presented in Table I. This table is a compilation of results from several references in which the comparison between comercial devices capable of measuring ACD_{post} is made. For each reference ACD_{post} was measured in a group of patients and the mean ACD_{post} was calculated as well as the associated standard deviation. The devices used in each study are listed in column *Devices* and the respective measurement technique in column *Technique*. References [9–11] found the devices tested to not be interchangeable. Results from reference [12] were found to be interchangeable, which is contradictory to reference [9] results. This set of results urges the need for investigation regarding the accuracy of ACD_{post} measuring techniques since this parameter plays a fundamental role in the refractive outcome of cataract surgery. Accurately measuring ACD_{post} is therefore crucial in the following situations:

- Validation of IOL position prediction methods;
- Possible improvement of the refractive outcome of the second eye when using ACD_{post} measurements of the first eye to calculate the IOL power.
- Ray tracing based methodologies which make a direct use of this parameter.

Device	Technique	Mean ± SD ACD_{post} (mm)	Reference
Tomey AL-2000	A-Scan Ultrasound	3.97 ± 0.45	[9]
Oculus Pentacam	Scheimpflug Imaging	3.41 ± 0.28	
Alcon Ocuscan Biometer	A-Scan Ultrasound	3.81 ± 0.41	[10]
Zeiss IOLMaster	Slit-beam Photography	4.06 ± 0.46	
Oculus Pentacam	Scheimpflug Photography	4.05 ± 0.58	
Zeiss Visante OCT	Optical Coherence Tomography	3.91 ± 0.29	[11]
OTI-Scan HF 35-50	Ultrasound Biomicroscopy	3.76 ± 0.33	
Alcon Ocuscan Biometer	A-Scan Ultrasound	4.54 ± 0.37	[12]
Grafton Optical Sirius	Scheimpflug Imaging	4.58 ± 0.34	

TABLE I: Compilation of works comparing ACD_{post} measurement techniques.

Moreover, several authors have tried to improve the existing IOL power calculation methodology by addressing the issue via ray tracing analysis, [13–16], making a direct use of ACD_{post} measurements and therefore benefiting from accurate ones. This represents a Physics based approach towards IOL power calculation, contrasting with the currently used Statistics based approach, which is inherently limited, since the derived formulas are mostly valid in the dataset from which they were derived, leading to the need of iterative corrections. This means that using a different biometric measurement technique for a parameter, even a more accurate one than the one used to derive the formula's constants, or non average eye parameters when compared to the dataset, negatively affect the prediction and degrade the outcome. A ray tracing based approach has several key advantages:

- Individual eyes can be modeled, nullifying the need for population studies as well as iteratively calculating corrective factors.
- Is applicable to non average and post-LASIK[3] eyes without performance degradation.
- Can provide a development platform for new types of IOLs.

The results were found to be very promising, being as accurate as current power calculation formulas.

III. CLINICAL STUDY

A. Patients and Methods

A clinical study involving 25 patients scheduled for phacoemulsification cataract surgery was conducted at Hospital da Luz. Preoperative biometry was performed with the Lenstar LS 900. The mean preoperative values (± standard deviation) for axial length and corneal power were:

- 23.24 ± 0.55 (mm)
- 43.84 ± 1.37 (D)

All surgeries were performed by the same surgeon whom implanted the same IOL model in every patient: a biconvex 22D Alcon AcrySof single-piece SA60AT. Most manufacturers do not disclose certain parameters regarding an IOL, such as the curvatures of the surfaces,

[3] LASIK is a very popular refractive surgery procedure, reshaping the cornea in order to achieve good vision quality.

sphericity, thickness and refractive index, which hinders progress related to this field as these parameters are needed for ray tracing and could also be useful for other applications [4]. For this particular IOL all parameters required for computational modeling were known, Table II, and as such it was chosen for this study.

3 months after surgery subjective visual acuity evaluation was performed. 20/20 vision was achieved in all patients with the best optical correction. ACD_{post} was measured 3 months postoperatively with both the Lenstar LS 900 and Zeiss Visante OCT. Lenstar failed to measure ACD_{post} 13% of the times, which resulted in the exclusion of these cases from the following analysis, reducing the sample size from 40 to $n = 35$ eyes.

Parameter	Value
Central Thickness (mm)	0.668
Anterior surface radius (mm)	16.379
Anterior surface asphericity	0
Posterior radius (mm)	25
Posterior surface asphericity	0
n (λ=555nm)	1.554
Abbe number	37

TABLE II: SA60AT parameters [17, 18].

B. ACD_{post}: Visante vs Lenstar

When assessing the comparability between measurements from different devices correlation analysis is not a suitable method since it analyzes the relationship between variables and not the differences between them [19]. On the other hand, Bland-Altman (BA) analysis is a very useful method of assessing if the measurements are comparable to the extent that one can replace the other for the intended purpose of the measurement [20], being widely used when comparing biometric measurements. The BA plot in Figure 2 displays the differences between paired measurements against their paired mean.

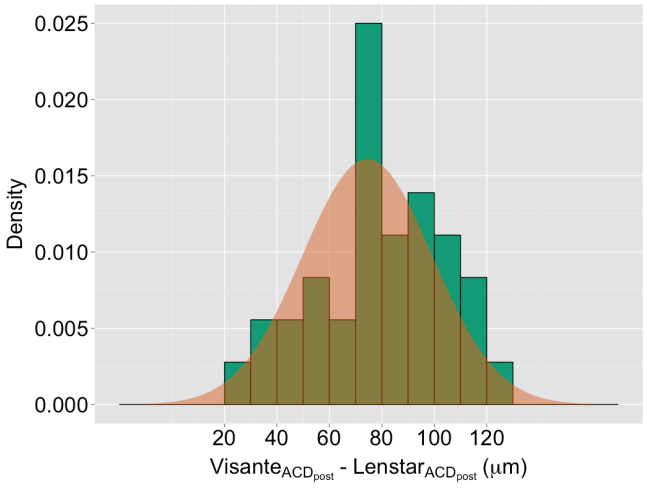

FIG. 1: Histogram of the differences.

The dashed line in the middle of the plot represents the mean difference, $\bar{d} = 74$ μm, while the other two represent the limits of agreement $\bar{d} \pm 1.96\sigma$, with $\sigma = 25$ μm. The confidence intervals for the mean and for both limits of agreement are presented in Table III and shaded in Figure 2.

Parameter	Confidence interval (μm)
$\bar{d}$ + 1.96 σ	[108; 138]
$\bar{d}$	[66; 83]
$\bar{d}$ - 1.96 σ	[11; 44]

TABLE III: Confidence intervals for the BA plot.

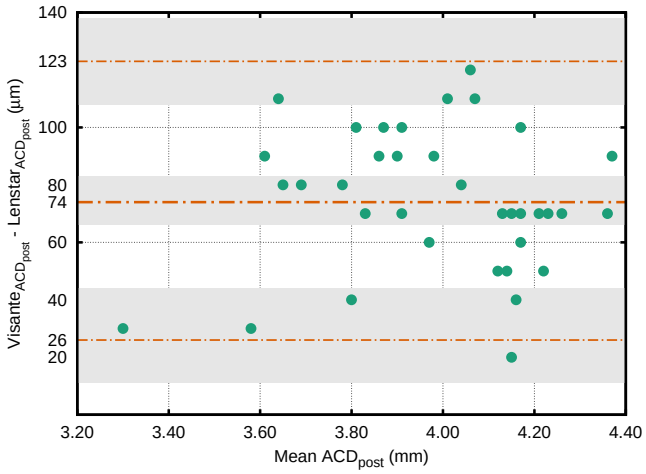

FIG. 2: BA plot of ACD_{post} measurements.

With this information it is possible to conclude that a systematic difference between the measuring devices exists: the Visante consistently makes larger ACD_{post} measurements. This does not provide information regarding:

- Interchangeability of the measurements. We need to assess the clinical significancy of the differences – that is, what is the consequence of using either measurement in an IOL power calculation formula, or what is the change in the final refraction of the patient considering an ACD_{post} shift of this magnitude;
- Accuracy of the measurements – only calibrations using physical references of known length can grant us a deeper insight on this matter. Since the devices share a common working principle it is plausible that both are committing the same systematic error and this has to be addressed.

In order to assess the clinical significancy of the differences the refraction on the spectacle plane, R_S, was calculated using geometrical optics formulas. The refractive shift at the spectacle plane was calculated for a normal and for an extreme eye, Table IV, considering a 138μm ACD_{post} shift from the optimum position (0D refraction at the spectacle plane), which corresponds to the upper limit of the confidence interval for the agreement of the measurements as presented in Table III. The normal eye parameters correspond to average population[4] values

[4] This data is not from the clinical trial. It refers to average population values found in references [21, 22].

while the extreme eye parameters correspond to average population values associated with 2 standard deviations. The IOL power of the normal eye was chosen to be the same of the IOL used in this work while the IOL power for the extreme eye was chosen to be abnormally large, so that the effect of the differences between measurements could be perceived more easily.

Eye	AL (mm)	R_1 (mm)	IOL (D)	$\bar{d} + 1.96\sigma$ Shift (D)
Normal	23.46	7.87	22	0.20
Extreme	21.40	8.41	34	0.35

TABLE IV: Effect of IOL shift on the spectacle plane refraction.

The normal eye has a refractive shift inferior to 0.25D, making it clinically insignificant, however the extreme eye does not. It should be noted however that the combination of parameters used to calculate this result is unlikely to be found in practice and that and we are using the upper limit of the confidence interval for the limits of agreement of the measurements. For this reason the refractive shift considering a difference equal to the upper limit of the confidence interval for the mean of the differences between devices, 83μm, Table III, was also calculated and found to be 0.18D, which is clinically insignificant.

These findings constitute a very strong indication that the results found are interchangeable. Although this is a good indicator that the measurements are being done correctly it is still necessary to assess their accuracy.

C. Lens Thickness

When performing postoperative biometry Lenstar is able to measure the thickness of the implanted IOL. The mean thickness ($\pm$ SD) was found to be 0.737 ± 0.078mm while the manufacturer indicates a thickness of $t_{IOL} =$ 0.668mm . Since the device measures the optical path, returning the physical distance d:

$$OP = n \cdot d, \tag{1}$$

it is possible that this discrepancy is due to a mismatch between the IOL's refractive index and the one used by the software to calculate the thickness. This hypothesis is investigated here.

The IOL's refractive index, $n_{\mathsf{IOL}}(\lambda = 555\mathsf{nm}) = 1.554$, has to be updated to consider dispersion since Lenstar's central wavelength is 820nm. The refractive index of the IOL for several wavelengths is not provided and was estimated using data from N. Sultanova et al., 2009, [23] and considered to be $n(\lambda = 820\mathsf{nm}) \simeq= 1.541$.

Therefore:

$$n_{\mathsf{IOL}}(\lambda = 820\mathsf{nm}) \cdot t_{\mathsf{IOL}} = n_{\mathsf{Lenstar}} \cdot d_{\mathsf{Lenstar}} \Rightarrow n_{\mathsf{Lenstar}} = 1.397. \tag{2}$$

For the values mean $\pm$ SD we find: $n_{\mathsf{Lenstar}} = 1.263$ and $n_{\mathsf{Lenstar}} = 1.562$. According to reference [24], the refractive indexes of IOLs vary between 1.42 and 1.55, and therefore it seems that an eventual refractive index mismatch is not the only reason for the present discrepancy.

IV. PSEUDOPHAKIC EYE PHANTOM

In order to assess the accuracy of $\mathrm{ACD}_{\mathrm{post}}$ measurements made by the Zeiss Visante OCT and the Haag-Streit Lenstar LS 900 in a life-like and realistic scenario a pseudophakic eye phantom was built, Figure 3. The phantom was built using laboratory grade optomechanical components, custom designed components and a 22D SA60AT Alcon AcrySof single-pice IOL, the same model implanted in all patients involved in the clinical trial. The phantom's construction is modular so it can be used with both devices.

The phantom consists of a 5cm tall top opened square shaped box, 4cm side length, with a plastic covered 12mm diameter circular aperture in one of its faces – acting as a flat cornea.

The IOL is installed in a custom IOL holder, which is glued onto a custom optical post that is in turn connected to off-shelf optical posts mounted on a translation stage.

The stage is actuated via a high precision micrometer head (5 μm/div), allowing for precise axial displacements relatively to the front surface.

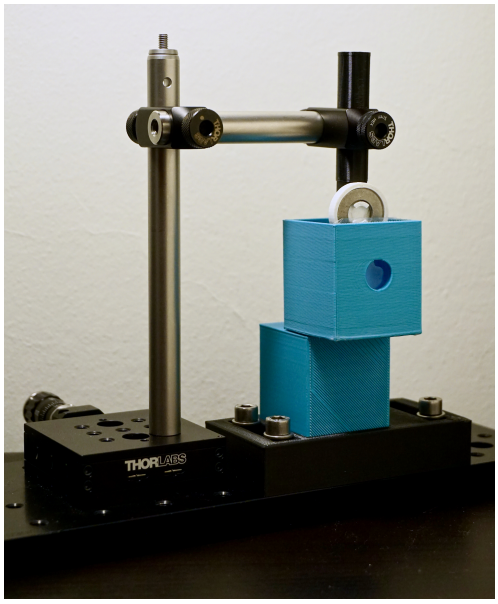

FIG. 3: Pseudophakic eye phantom. Clamping system not pictured.

A. Results

Both devices measure the physical distance, d, through the optical path, $d = OP/n$, with n being the refractive index of the aqueous humor considering the dispersion caused by the light source's central wavelength:

- $\lambda_0 = 820\mathsf{nm}$ for the Lenstar.
- $\lambda_0 = 1310\mathsf{nm}$ for the Visante,

When air is inside the box this has to be accounted for as the results presented by the devices for ACD_{post} are divided by the refractive index of the aqueous. Data obtained by P. Schiebener et al., 1990, [25] regarding the refractive index of water for several combinations of wavelengths and temperatures was interpolated to find the refractive index for both devices at 37C and 1MPa:

- $n(\lambda_0 = 820\text{nm}) = 1.32614$
- $n(\lambda_0 = 1310\text{nm}) = 1.32089$

These values were used to multiply the measurements presented by the device when the box was air filled.

The relative displacements measured were fitted to the linear equation:

$$\Delta_{\text{Device}} = \Delta_{\text{Phantom}} \cdot a + b, \tag{3}$$

and the fit parameters a and b were calculated using Gnuplot's least squares fitting feature. Ideally $a = 1$ and $b = 0$.

The micrometer head used has a reported sensitivity of 1μm and the divisions are 5 μm apart. As such, its error is considered to be negligible. Both devices present the measurements in mm with two decimal places, therefore the measurement uncertainty was considered to $\delta_m = 5\mu$m. For the differences this was propagated, $\delta\Delta_{\text{Device}} = \sqrt{2}\delta_m$.

Doing a calibration using relative displacements is not an effective way to check for the existence of a zero shift error since errors of this type affect all measurements equally and doing subtractions between absolute measurements may nullify its presence. It's therefore necessary to measure a physical reference of known length, in this case the IOL's thickness, to check for the presence of a zero shift error. Span shift errors can still be effectively detected with this type of calibration.

1. *Zeiss Visante Calibration*

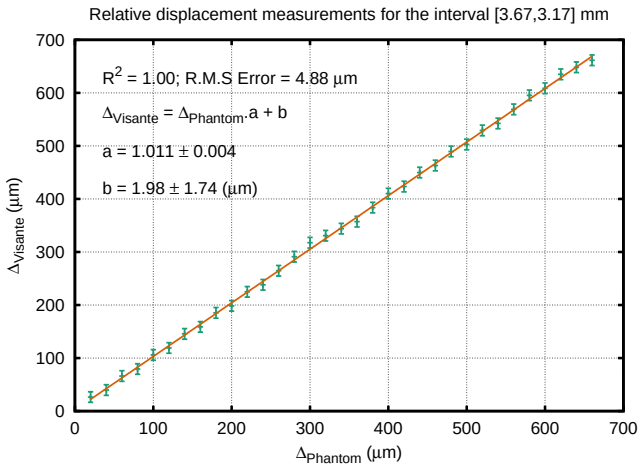

FIG. 4: Medium range measurements in air.

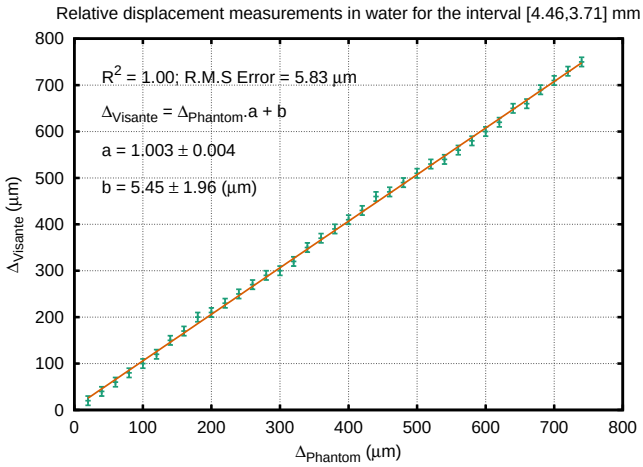

FIG. 5: Medium range measurements in water.

The results presented here were obtained for 20μm displacements of the IOL in air and water.

In Figure 4 relative displacement experimental data obtained with air inside the box is presented. Experimental data with water inside the box is presented in Figure 5 relative displacement. The R.M.S errors of the fits were found to be smaller than the device's 18 μm resolution in all the measurement sets. The fit parameters, a and b are also very close to the ideal value.

2. *Zeiss Visante IOL Thickness Measurement*

Visante uses the refractive index of the aqueous humor, $n_{\text{aq}}(\lambda = 1310\text{nm}) \simeq 1.323$, to convert optical path measurements into physical distances. Due to this the IOL thickness measured by the Visante, t_{Visante}, won't the match the IOL's physical thickness, 0.668mm. As such it is necessary to calculate the value of the measurement using the correct refractive index. The optical path was calculated via:

$$OP = t_{\text{Visante}} \cdot n_{\text{aq}}, \tag{4}$$

and the IOL's thickness was then calculated from:

$$t_{\text{IOL}} = OP/n_{\text{IOL}}(\lambda = 1310\text{nm}). \tag{5}$$

The IOL's refractive index was estimated to be $n(\lambda = 1310\text{nm}) \simeq 1.535$. using data obtained by N. Sultanova et al., 2009, [23].

The central thickness corresponds to the thickest point of the lens and since it is difficult to exactly pinpoint several tomograms were acquired in different regions of the IOL. At the thickest point the value found was 0.61mm, having a 56μm deviation from the expected value, 0.668mm. It's important to consider how IOL manufacturing tolerances affect this result. Current fabrication technologies allow IOLs to be fabricated with a $\pm 5\mu$m center thickness tolerance [26]. Assuming the tolerance of the IOL used to be five times this value the difference becomes $56 \pm 25\mu$m. A measuring error of this magnitude is negligible, as previously found, see Table IV results.

3. *Haag-Streit Lenstar Calibration*

This device allows measurements to be made along longer ranges and for this reason 50μm IOL displacements were made, as seen in Figure 6. The fit parameters obtained were $a = 1.017 \pm 0.003$ and $b = -17.17 \pm 5.10 \mu$m. The R.M.S error is 18.32 μm.

It is therefore important to check if the device accurately measures ACD_{post} when water is inside the box and for this reason acquisitions with 20μm displacements were made, Figure 7. Fit parameters of $a = 1.054 \pm 0.022$ and $b = 4.25 \pm 4.74$ μm were found, as well as a R.M.S error of 9.64μm.

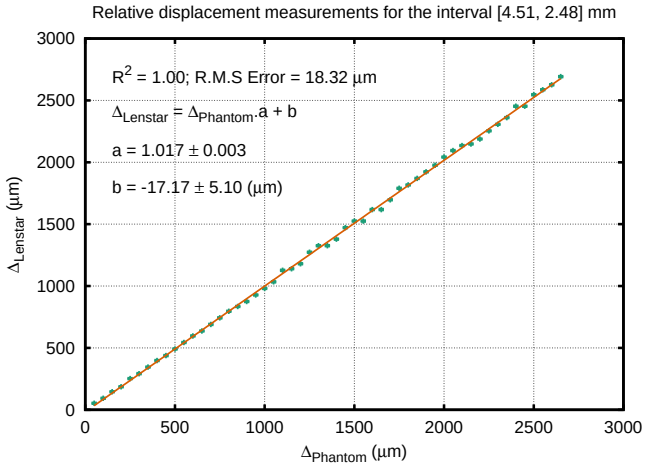

FIG. 6: Medium range measurements in air.

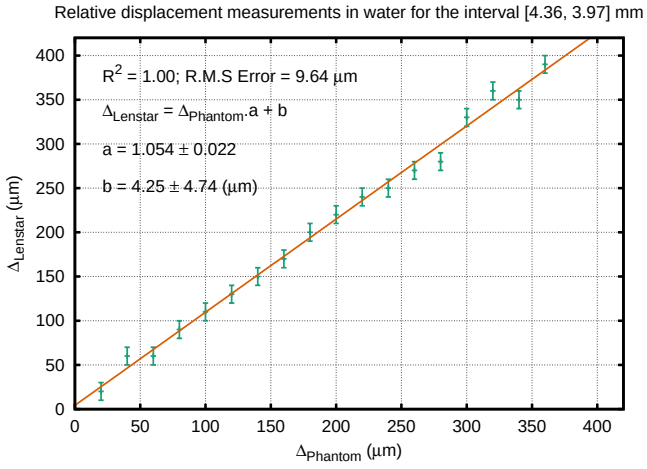

FIG. 7: Medium range measurements in water.

4. *Validity of the Results*

It is important to consider the effect of tilts and decentration between the IOL and the cornea and between the cornea and the measuring devices on the quality of the measurements.

Considering that the devices' effectively measure the reflectivity profile of a sample the existence of a tilt reduces the intensity of the back reflected signal, degrading the image quality. A decentered IOL in relation to the measuring beam also reduces the intensity of the back reflected signal from its surface as this is stronger when the beam impinges on the vertex.

The IOL has several degrees of freedom: it can be moved axially via the micro-metric stage, the height can be adjusted, and it can be tilted in relation to the cornea. Due to the reasons previously explained the IOL was visually aligned with the cornea, so that the measuring conditions were close to optimal, maximizing the back reflected signal's strength.

The cornea is flat and as such it is not affected by decentration. When the phantom was clamped to the devices it was possible to observe that it was mostly perpendicular to incoming beam, which maximizes the reflection.

It's important to note that eventual existence of a tilt does not invalidate the measurements obtained: the alignment of the devices with the cornea and the alignment of the IOL with the cornea was performed before making each measurement set, so every measurement from the same set is made in the same conditions.

Measurements with the phantom were all made by the same operator and as such it is not possible to draw any conclusion regarding the inter-operator reproducibility, which is an important aspect to consider. Inter-operator reproducibility of ACD_{post} measurements obtained with the Visante OCT was evaluated by Qi Zang et al. in 2010 [11] and the results were found to good. In this work ACD_{post} was measured in 25 pseudophakic eyes by two operators and mean values $\pm$SD of 3.810 $\pm$ 0.297 mm and 3.801 $\pm$ 0.293 mm were found. These findings support that the fact that measurements obtained with the Zeiss Visante are operator independent. The findings made with the phantom regarding the calibration of the Visante, specifically when the box contained water, paired with the measurement of the thickness of the IOL provide a very strong indication that the device is capable of accurately measuring ACD_{post} in pseudophakic eyes.

Results obtained through the clinical study show that results obtained with the Haag-Streit Lenstar are interchangeable with the ones of the Zeiss Visante, however inter-operator reproducibility of ACD_{post} measurements obtained with the Haag-Streit Lenstar has not been assessed in the literature. Moreoever, this device had issues regarding accurate measurement of the IOL thickness in vivo, which is probably due to the difficulty in detecting the reflection from its posterior surface combined with an eventual mismatch of the refractive index of the IOL. It is important to beware that an accurate IOL thickness measurement will propagate its error to posterior eye structures which impacts the accuracy of axial length measurements. As such, performing biometry with this device in pseudophakic eyes will likely result in incorrect axial length measurements. When using the eye phantom the performance of this device was also found to be inferior to the one of the Visante.

V. PERSONALIZED PSEUDOPHAKIC EYE MODEL

Liou-Brennan's eye model was implemented and used in conjunction with biometric data collected during the clinical study to calculate $\mathrm{ACD_{post}}$ in each case. The biometric parameters presented in Table V were used to personalize the model.

Parameter	Represented by
Central Corneal Thickness	CCT
Anterior Corneal Radius	$\mathrm{R_1}$
Crystalline Thickness	LT
Axial Length	AL

TABLE V: Biometric parameters used in the personalized eye model.

1. Corneal Radius

Lenstar calculates the anterior corneal radius through keratometry, averaging the corneal power along two perpendicular meridians:

$$P = \frac{1}{\mathrm{R_1}} \cdot (n_a - n_0), \tag{6}$$

where P is the average corneal power, $n_0 = 1$ the air's refractive index and $n_a = 1.3375$ the combined refractive index of the cornea and of the aqueous humor. For modeling purposes $\mathrm{R_2}$ is obtained considering a ratio between the surfaces,

$$\mathrm{R_2} = k \cdot \mathrm{R_1}, \tag{7}$$

where k is the ratio between the corneal curvatures of an eye model. This is a similar approach to the one used in reference [15], however in this case the values from the Liou-Brennan eye model were used:

$$k = \frac{6.4}{7.77}. \tag{8}$$

This method does not take into account intrinsic corneal astigmatism.

2. Corneal Asphericity

Since no corneal topography data was available and no relation between corneal asphericity and other parameters is known the best option was to use nominal population values for these parameters. For this reason the asphericities were considered to be $Q_1 = -0.18$ and $Q_2 = -0.60$.

3. Postoperative Refraction

Posteoperative refraction was implemented using the postoperative subjective visual acuity via thin lens approximation. The spherical equivalent power of the prescribed refraction, S_{eq}, was used to calculate the spectacle lens radius considering a polycarbonate glass.

4. Implementation

Custom glasses were created for both the cornea and the aqueous humor. For the IOL the respective refractive index and Abbe number were used.

The location of the pupil was not measured and as such the position of the Liou-Brennan eye model was used. The surface named *Free space* is the gap between the IOL and the pupil and has a variable, non-user defined, z thickness which is calculated by optimizing the optical system. The last surface's thickness depends on the latter's, as can be seen in Table VI, keeping the axial length of the eye constant. This allows to calculate the IOL position using the postoperative refraction. It is also interesting to calculate the spectacle plane refraction using experimental $\mathrm{ACD_{post}}$ measurements and optimizing the radius of the spectacles, r, as seen in Table VII.

#	Surface	R (mm)	t (mm)	Q	Glass
1	Object	∞	6000	0	Air
2	Spectacles	S_{eq}	1	0	Polycarbonate
3	Object	∞	12	0	Air
4	Cornea anterior	R_1	CCT	-0.18	Cornea
5	Cornea posterior	R_2	3.16	-0.60	Aqueous Humor
6	Pupil	∞	0	0	Aqueous Humor
7	Free space	∞	z	0	Aqueous Humor
8	IOL Front	16.379	CT	0	IOL
9	IOL Back	-25	AL $-$ (CCT + CT + 3.16 + z)	0	Aqueous Humor

TABLE VI: Implementation of the personalized eye model: $\mathrm{ACD_{post}}$ optimization.

#	Surface	R (mm)	t (mm)	Q	Glass
1	Object	∞	6000	0	Air
2	Spectacles	r	1	0	Polycarbonate
3	Object	∞	12	0	Air
4	Cornea anterior	R_1	CCT	−0.18	Cornea
5	Cornea posterior	R_2	3.16	−0.60	Aqueous Humor
6	Pupil	∞	0	0	Aqueous Humor
7	Free space	∞	$\text{ACD}_{\text{post}} - 3.16$	0	Aqueous Humor
8	IOL Front	16.379	CT	0	IOL
9	IOL Back	−25	$\text{AL} - (\text{CCT} + \text{CT} + 3.16 + z)$	0	Aqueous Humor

TABLE VII: Implementation of the personalized eye model: refraction optimization.

A. Merit Function and Vision Quality Metric

The merit function is used to optimize the designed optical system given a set of variable parameters, in this case, ACD_{post} or the radius of the spectacle plane. The Visual Strehl ratio calculated in the Modulation Transfer Function domain (VSMTF) image quality metric has a correlation coefficient of $\text{R}^2 \simeq 0.73$ with subjective vision quality, [27], and served as a basis for the implemented merit function.

In a visual acuity test the patient identifies letters, which are composed of both horizontal and vertical stripes. For this reason the average MTF operand (MTFA) was used for the merit function. The targets of the MTFA operand were chosen to be the average MTF frequencies of the Liou-Brennan eye with the weight being the corresponding Contrast Sensitivity Function (CSF) value for that frequency. Eight MTFA operands were used in the metric function – a compromise between computational speed and accuracy.

VI. RESULTS

In order to analyze the impact of the merit function and of the pupil diameter on the ability to predict ACD_{post} an extensive battery of tests was made, with the results being summarized in Table VIII. This table presents the mean absolute different and standard deviation between ACD_{post} measurements from the Visante and those obtained from the simulations. Since the failure rate of the Lenstar reduced the sample size and the devices were proven to be interchangeable in the previous section comparisons were only made between the Visante device measurements and the simulations. The *Simulation* column refers to different combinations of merit function and applied refractive correction. The column *Zemax Pupil Diameter* refers to the pupil diameter of the modeled eyes – since this parameter was not measured for each patient simulations were made for 3 diameters.

Simulations A, B and C were made using a merit function with MTFA targets of a 4mm pupil. There is little difference between results of simulation A and B and only when the spherical equivalent refractive, simulation C, correction is applied we see a significant improvement.

Simulations D and E were made using a merit function with MTFA targets of a 5mm pupil. Comparing the results obtained with this pupil size with those of the 4mm pupil, the difference is not significant, although better results were obtained for targets of the 5mm pupil diameter.

Results from simulation E were found to be in better agreement with experimental data than the rest, having both the lowest mean absolute difference and standard deviation. Simulation E uses the VSMTF based merit function with MTFA targets of the for a 5mm diameter pupil Liou-Brennan eye. In this simulation the subjective spherical equivalent postoperative refractive error correction was applied for each patient.

Simulation	Zemax Pupil Diameter (mm)	Mean Absolute Difference (mm)	σ (mm)
A	2	0.416	0.453
	3	0.394	0.474
	4	0.447	0.485
B	2	0.439	0.470
	3	0.417	0.444
	4	0.487	0.463
C	2	0.352	0.385
	3	0.331	0.380
	4	0.379	0.388
D	2	0.511	0.539
	3	0.494	0.492
	4	0.498	0.488
E	2	0.313	0.377
	3	0.270	0.347
	4	0.358	0.381

TABLE VIII: Simulations' results with VSMTF based merit function using MTFA targets of the Liou-Brennan eye with:
A - 4mm pupil, uncorrected refractive error; B - 4mm pupil, spherical refractive error correction;
C - 4mm pupil, spherical equivalent refractive error correction; D - 5mm pupil, uncorrected refractive error;
E - 5mm pupil, spherical equivalent refractive error correction;

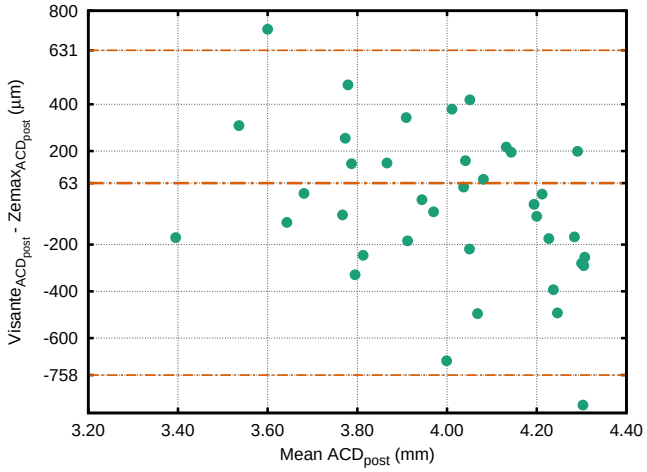

FIG. 8: BA plot of ACD_{post} for simulation E.

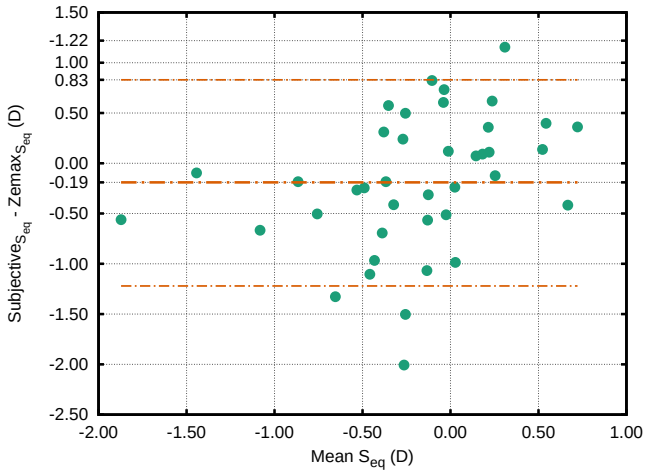

FIG. 9: BA plot of the S_{eq} for simulation E.

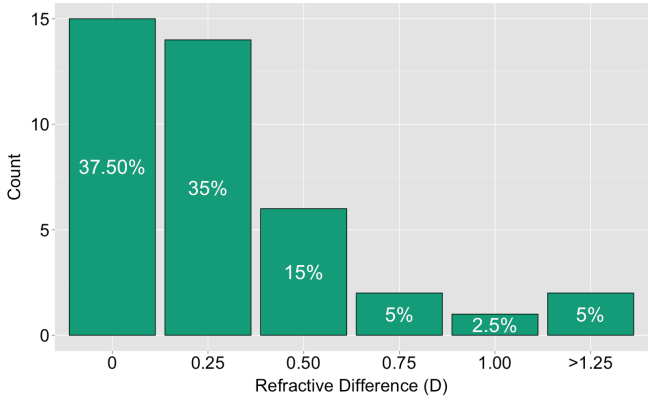

FIG. 10: Bar chart of the differences in diopters.

Simulation E results are presented in Figure 8 in the form of a BA plot, being possible to observe that an obvious relationship between the differences and ACD_{post} does not exist. The mean difference line ($\bar{\mu}$ =63μm) is dash plotted, as well as the limits $\bar{\mu} \pm 2\sigma$.

Refraction at the spectacle plane was also calculated through optimization using simulation E conditions and the ACD_{post} measured with the Visante, Figure 9. These results are presented as a bar chart in Figure 10. 37.5% of the cases have a refractive difference smaller than 0.25D, which is not clinically significant. The rest of the differences are significant.

VII. FINAL REMARKS

The main purpose of this work was the assess the capability of accurately measuring ACD_{post} using devices commonly found in ophthalmological clinics.

The clinical study conducted gave us a clear indication that the devices under study, Lenstar LS 900 and Visante OCT, are interchangeable, and, thanks to the experimental work developed with the phantom, indeed accurate, with the Visante having a superior performance. The span shift error of this device is virtually non existent and the IOL thickness was measured with a 56 $\pm$ 25μm error, which, if considered to be the zero shift error is clinically insignificant. The Lenstar device would sometimes become uncooperative, not providing an ACD_{post} measurement, probably due to the fact the reflection from the frontal surface of the IOL is too dim, being regarded as noise by the software. On the other hand, the Visante OCT always provides tomographic images and even when the frontal surface of the IOL is not fully rendered the user can still measure its position accurately. So if the two devices are available, and the parameter of interest is ACD_{post}, the Visante OCT seems to be the best option. Only one IOL model was used during this work and it was possible to make accurate measurements with both devices. These results are valid for other IOLs as long as its reflective properties are similar to the one used in this work, however, due to the great number of IOLs available in the market this should be analyzed.

Knowing that interferometry based devices perform accurate measurements of ACD_{post} will certainly contribute to improve ELP estimation methodologies and continue to push forward ray tracing based methodologies, which make a direct use of the ACD_{post}.

Regarding the computational work two important factors should be highlighted:

- Approximations regarding the shape of the anterior cornea and position of the pupil.
- Aspects related to the optimization procedure.

The anterior cornea was modeled as a conicoid. This approximation disregards intrinsic corneal astigmatism. Moreover asphericity was not measured during the clinical trial so the average population value for this parameter was used. Using corneal topography to implement the shape of the cornea is likely to improve the results. Moreover, subjective refraction was used to calculate the spherical equivalent power. If using corneal topography it is necessary to implementing toric lenses for astigmatism correction. While performing the simulations the pupil position reveled itself to be critical for the optical performance of the eye and, since this parameter was not measured, a population value for this parameter was used.

The optimization procedure consisted in using MTF values of the Liou-Brennan eye for both 4mm and 5mm

pupils while weighting these values with the CSF. These targets refer to average phakic eyes and the MTF performance of a pseudophakic eye is different since the IOL does not compensate corneal aberration as well as a human crystalline. Using targets from pseudophakic eyes would likely improve the results.

Despite these approximations the results obtained via ray tracing are on par as the ones obtained with current IOL power calculation formulas (90% of patients within ± 1D of the target refraction). It should be noted however, the the patient subset used in this work was compromised of average eyes, which was a consequence of using cases implanted with the same 22D IOL model. Nonetheless ray tracing is a very powerful tool and in the future it is very likely to be used to improve the refractive outcome of cataract surgery.

[1] World Health Organization. Prevention of Blindness and Visual Impairment. `http://www.who.int/blindness/causes/priority/en/index1.html`, 2015. [Online; accessed 12-October-2015].

[2] Petros Aristodemou, Nathaniel E Knox Cartwright, John M Sparrow, and Robert L Johnston. Formula choice: Hoffer Q, Holladay 1, or SRK/T and refractive outcomes in 8108 eyes after cataract surgery with biometry by partial coherence interferometry. *Journal of Cataract & Refractive Surgery*, 37(1):63–71, 2011.

[3] Garry Brian and Hugh Taylor. Cataract blindness: challenges for the 21st century. *Bulletin of the World Health Organization*, 79(3):249–256, 2001.

[4] Thomas Olsen. Calculation of intraocular lens power: a review. *Acta Ophthalmologica Scandinavica*, 85(5):472–485, 2007.

[5] Douglas J Covert, Christopher R Henry, and Steven B Koenig. Intraocular lens power selection in the second eye of patients undergoing bilateral, sequential cataract extraction. *Ophthalmology*, 117(1):49–54, 2010.

[6] Thomas Olsen. Use of fellow eye data in the calculation of intraocular lens power for the second eye. *Ophthalmology*, 118(9):1710–1715, 2011.

[7] Valliammai Muthappan, Daniel Paskowitz, Ava Kazimierczak, Albert S Jun, John Ladas, and Irene C Kuo. Measurement and use of postoperative anterior chamber depth of fellow eye in refractive outcomes. *Journal of Cataract & Refractive Surgery*, 41(4):778–784, 2015.

[8] Petros Aristodemou, Nathaniel E Knox Cartwright, John M Sparrow, and Robert L Johnston. First eye prediction error improves second eye refractive outcome: Results in 2129 patients after bilateral sequential cataract surgery. *Ophthalmology*, 118(9):1701–1709, 2011.

[9] Gabor Nemeth, Attila Vajas, Bence Kolozsvari, Andras Berta, and Laszlo Modis. Anterior chamber depth measurements in phakic and pseudophakic eyes: Pentacam versus ultrasound device. *Journal of Cataract & Refractive Surgery*, 32(8):1331–1335, 2006.

[10] Po-Fang Su, Andy Y Lo, Chao-Yu Hu, and Shu-Wen Chang. Anterior chamber depth measurement in phakic and pseudophakic eyes. *Optometry & Vision Science*, 85(12):1193–1200, 2008.

[11] Qi Zhang, Wanqing Jin, and Qinmei Wang. Repeatability, reproducibility, and agreement of central anterior chamber depth measurements in pseudophakic and phakic eyes: optical coherence tomography versus ultrasound biomicroscopy. *Journal of Cataract & Refractive Surgery*, 36(6):941–946, 2010.

[12] Giacomo Savini, Kenneth J Hoffer, and Michele Carbonelli. Anterior chamber and aqueous depth measurement in pseudophakic eyes: Agreement between ultrasound biometry and scheimpflug imaging. *Journal of Refractive Surgery*, 29(2):121–125, 2013.

[13] Haiying Jin, Tanja Rabsilber, Angela Ehmer, Andreas F Borkenstein, Il-Joo Limberger, Haike Guo, and Gerd U Auffarth. Comparison of ray-tracing method and thin-lens formula in intraocular lens power calculations. *Journal of Cataract & Refractive Surgery*, 35(4):650–662, 2009.

[14] Keiichiro Minami, Yasushi Kataoka, Jiro Matsunaga, Shinichiro Ohtani, Masato Honbou, and Kazunori Miyata. Ray-tracing intraocular lens power calculation using anterior segment optical coherence tomography measurements. *Journal of Cataract & Refractive Surgery*, 38(10):1758–1763, 2012.

[15] Thomas Olsen and Mikkel Funding. Ray-tracing analysis of intraocular lens power in situ. *Journal of Cataract & Refractive Surgery*, 38(4):641–647, 2012.

[16] Maria Filomena Jorge Ribeiro. *Personalized pseudophakic model*. PhD thesis, Instituto Superior Técnico, 2013.

[17] Sergio Barbero, Susana Marcos, Javier Montejo, and Carlos Dorronsoro. Design of isoplanatic aspheric monofocal intraocular lenses. *Optics express*, 19(7):6215–6230, 2011.

[18] Huawei Zhao and Martin A Mainster. The effect of chromatic dispersion on pseudophakic optical performance. *British journal of ophthalmology*, 91(9):1225–1229, 2007.

[19] Davide Giavarina. Understanding bland altman analysis. *Biochemia medica*, 25(2):141–151, 2015.

[20] Douglas G Altman and J Martin Bland. Measurement in medicine: The analysis of method comparison studies. *The statistician*, pages 307–317, 1983.

[21] Michiel Dubbelman, Henk A Weeber, Rob GL Van Der Heijde, and Hennie J Völker-Dieben. Radius and asphericity of the posterior corneal surface determined by corrected scheimpflug photography. *Acta Ophthalmologica Scandinavica*, 80(4):379–383, 2002.

[22] Renu Jivrajka, Maya C Shammas, Teresa Boenzi, Mike Swearingen, and H John Shammas. Variability of axial length, anterior chamber depth, and lens thickness in the cataractous eye. *Journal of Cataract & Refractive Surgery*, 34(2):289–294, 2008.

[23] N Sultanova, S Kasarova, and I Nikolov. Dispersion properties of optical polymers. *Acta Physica Polonica-Series A General Physics*, 116(4):585, 2009.

[24] Roberto Bellucci. *An introduction to intraocular lenses: material, optics, haptics, design and aberration*. Karger Publishers, 2013.

[25] P Schiebener, Johannes Straub, JMH Levelt Sengers, and JS Gallagher. Refractive index of water and steam as function of wavelength, temperature and density. *Journal of physical and chemical reference data*, 19(3):677–717, 1990.

[26] Benz R&D, Optical Blocker. `http://benzrd.com/ilt_optical_blocker.php`, 2016. [Online; accessed 12-April-2016].

[27] J.D. Marsack, L.N. Thibos, R.A.Applegate. Metrics of optical quality derived from wave aberrations predict visual performance. *Journal of Vision*, 2004.